γmean(19vs37cp)=0.7±0.1, γmean(19vs73cp)=0.6±0.1 and γmean(37vs73cp)=0.6±0.1. The cumulated iQM signal coincided with 2D ionchamber array measurements and demonstrated accurate reproducibility for all three plans (figure 1b). The control-point resolved analysis (fig.1c) consistently indicated large deviations between 19cp, 37cp and 73cp plans due to an imprecise data sampling synchronization of the preclinical version of the detector. The symmetry of the test plan could not be reflected by the iQM system, especially regarding the 19cp plan.
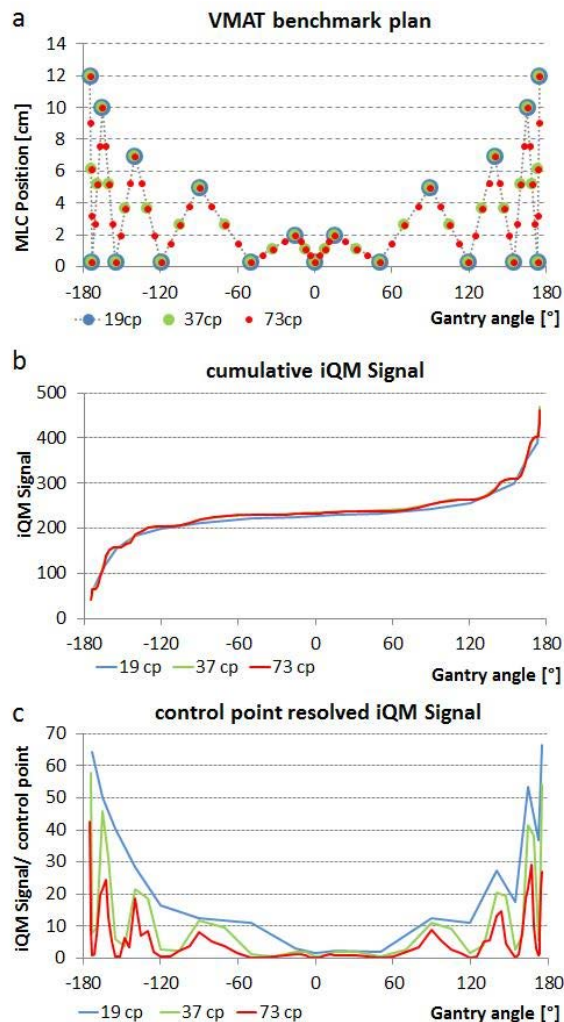
Conclusion: Increasing the number of control-points changed VMAT delivery accuracy marginally. For clinical treatment plans this effect might not be noticeable. Observation of the cumulative iQM signal coincided well with dosimetric measurements. The VMAT benchmark plan proved to be a prospective tool for visualizing and understanding linac and detector limitations.

EP-1562
VMAT pre-treatment verification using Octavius 4D system: from simple to more complex plans
H. Aslian[2], M. Severgnini[1], F. Cupardo[1], R. Vidimari[1], M. De Denaro[1]
[1]AOU "Ospedali Riuniti di Trieste", Medical Physics, Trieste, Italy
[2]International Center for Theoretical Physics and Trieste University, Medical Physics, Trieste, Italy

Purpose or Objective: Plan verification in complex treatment delivery techniques such as IMRT and VMAT is imperative. Although some studies have been conducted on pre-treatment VMAT quality assurance using PTW Octavius 4D systems, more works are needed to focus on complex VMAT plans including steep gradient regions. The aim of this study is to evaluate dose delivery of different VMAT plans such as Head and Neck (SIB: Simultaneously Integrated Boost), lung (SBRT: Stereotactic Body Radiation Therapy) and prostate (Hypo-fractionated intensity modulated arc therapy) with the Octavius 4D system.

Material and Methods: Fifteen head and neck, lung and prostate VMAT plans for fifteen patients (5 patients for each case) were created and their respective QA plans were calculated. All plans were optimized and calculated using Monaco (version 5.0) treatment planning system, which is a Monte Carlo-based treatment planning system. The 2D-array seven29, which consists of 729 vented plane-parallel ionization chambers arranged in a 27 x 27 matrix with the spatial resolution of 10mm, embedded in Octavius 4D cylindrical phantom was used to measure the dose distribution and the measurements were done with an Elekta Synergy linear accelerator equipped with an Agility 160 MLC system. In order to reconstruct and analyze the measured 3D dose from each plan, the PTW VeriSoft patient plan verification software was used and a volumetric 3D gamma index analysis for both 3%/3mm and 2%/2mm criteria was performed to compare and evaluate the measured and calculated doses. In addition, in order to improve the spatial resolution in cranial caudal direction due to 1 cm gap across the chambers the second measure was done by shifting the array 5 mm (via couch shift) in caudal direction and merging the matrices with the "merge" function available in PTW VeriSoft.

Results: The mean pass rate of volumetric 3D gamma index for all prostate cases was superior to 97% with 3%/3mm and 92% with 2%/2mm criteria. However, the mean passing rate for lungs was lower than prostate and ranged from 93.7 to 96.3 (3%/3mm) and from 90 to 94.1 (2%/2mm). Expectedly, the mean value of global gamma index for head and neck cases could not be better than 91.5% (ranged from 88.4 to 96.3) and 87.3% (ranged from 82.3 to 89) for the 3%/3mm and 2%/2mm criteria respectively. Also, merged measurements could increase the mean passing rate from 1% up to 3.5% in some complex cases (Fig.1).
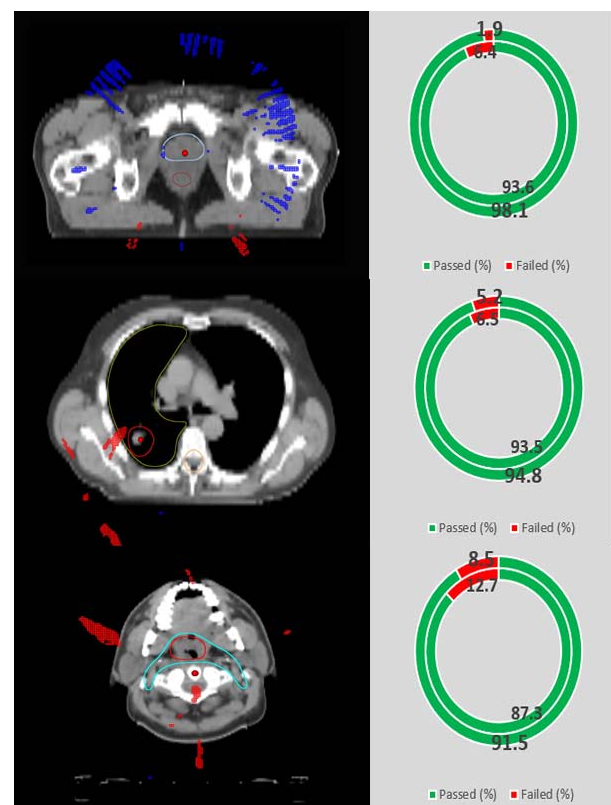

Fig. 1: The images (Left side) represent the failed points of a sample; The images (Right side) depict the average volumetric gamma index for prostates, lungs and HN cases in

which the outer pie-charts show the results with 3%/3mm and the inner pie-charts illustrate results with 2%/2mm.

Conclusion: The results showed that Octavius 4D phantom, with 2D-Array seven29, can be an adequate verification system both for simple and more complex cases. Additionally, the merge capability of the VeriSoft software, which can increase spatial resolution, is a useful tool for more complex VMAT plans.

EP-1563
Study of the characteristic of enhanced dynamic wedged depth dose profiles in non-homogenous media
A. Hussain[1], A. Zaman[2], M.B. Kakakhel[2]
[1]Aga Khan University Hospital, Department of Oncology, Karachi, Pakistan
[2]PIEAS, Department of physics and applied mathematics, Islamabad, Pakistan

Purpose or Objective: The aim of this study is to utilize the EGSnrc based Monte Carlo code in order to assess the EclipseTM (AAA) calculated dose estimation at the Water-Lung (WL) interfaces when irradiated by 6 MV photon beams at $15°$, $30°$, $45°$ and $60°$ wedge angles and multiple field sizes of 5 × 5 cm2, 10 × 10 cm2 and 20 × 20 cm2.

Material and Methods: EGSnrc sub codes are used for Monte Carlo dose simulation. BEAMnrc is used to simulate the linear accelerator head, whereas DOSXYZnrc is employed to perform phantom dose estimation. For simulating dynamic wedges the BEAMnrc component module DYNJAWS was employed. Phantom geometry includes a 10 cm layer of lung (r=0.250 g/cc) sandwiched between 5 cm and 10 cm water layers. Doses were calculated in exactly the same geometry and same density distribution by Monte Carlo and AAA algorithm. The overall dimension of the phantom was 30 cm × 30 cm × 25 cm. A 5 mm grid size (voxel width) along depth was used for calculating PDDs. The nominal source to surface distance (SSD) of 100 cm was used in both setups.

Results: The dose perturbation effect was found to be field size dependent. It increases with decreasing field size. No clear dependence for the wedge angles was observed. No dose deviation between AAA and EGSnrc was observed at the water→tissue interface. However a lower dose in the lung was estimated by AAA. Whereas at the lung→tissue junction a highest dose discrepancy was observed by AAA, estimating higher dose towards the water layer.
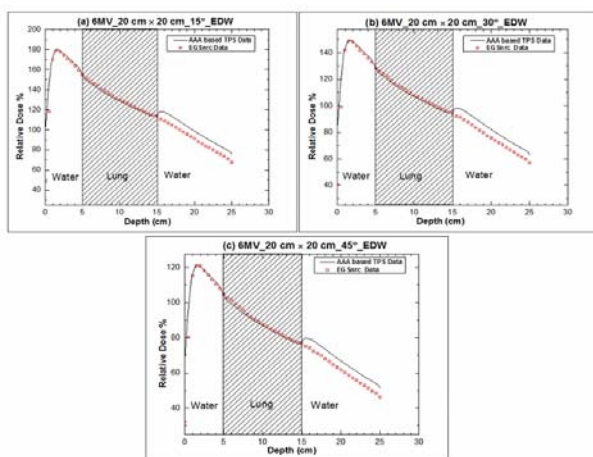
Conclusion: We have demonstrated the limitation of AAA in dose calculation at the water-tissue-water interfaces for four wedge angles. There was no significant wedge angle dependence on the dose perturbation. However an increase in perturbation was observed with decreasing field sizes for all angles.

EP-1564
Impact of dose calculation algorithm on SBRT and normofractionated lung radiotherapy in breath hold
M. Josipovic[1,2], G. Persson[1], J. Rydhög[1,2], J. Bangsgaard[1], L. Specht[1,3], M. Aznar[1,2]
[1]Rigshospitalet, Dept. of Oncology- Section for Radiotherapy, Copenhagen, Denmark
[2]University of Copenhagen, Niels Bohr Institute, Copenhagen, Denmark
[3]University of Copenhagen, Faculty of Medical Sciences, Copenhagen, Denmark

Purpose or Objective: Modern dose calculation algorithms only model absence of lateral charged particle equilibrium to a limited extent. The resulting uncertainties are largest in strongly heterogeneous regions, such as the thorax, and will potentially increase in deep inspiration breath hold (DIBH) due to decreased lung tissue density.

Material and Methods: Ten patients with stage I and ten with stage III lung cancer were included. For all patients, a plan in free breathing (FB, based on midventilation) and in DIBH were made with the clinically used Anysotropic Analytical Algorihtm (AAA). Stage I disease was treated stereotactically (SBRT) using 3D conformal technique (9-10 fields), 45 Gy in 3 fractions, prescribed to 95% isodose covering 95% of PTV and aiming for 140% dose in the isocenter. Stage III disease was treated with VMAT (2 arcs), 66 Gy in 33 fractions, prescribed to mean PTV dose. 6 MV energy was used for all plans. Calculation grid size was 1 mm for stage I and 2.5 mm for stage III. Plans were recalculated in more advanced Acuros with same MU as in AAA.
Plans were compared for target coverage (GTV, CTV, PTV), estimated from mean dose, near minimum (D98) and near maximum doses (D2), as defined in ICRU 83, and for SBRT also for the fraction of PTV covered by prescription dose (V45). Organs at risk parameter for stage I was fraction of lung receiving more than 13 Gy (V13), and for stage III, mean lung dose, lung V5, V20 and V40 and also mean heart dose and heart V50.

Results: In DIBH, lung density decreased by median 6% (47.6 HU) reduction for stage I and 12% (88.5 HU) for stage III.
In stage III, AAA overestimated mean target doses for FB and DIBH GTV and DIBH CTV (by median <0.8 Gy; p<0.05 Wilcoxon signed-rank test) and had no impact on D2. AAA overestimated D98 by median ~1 Gy for GTV and CTV (p<0.05), and more for PTV (by 1.5 Gy and 2.1 Gy, in FB and DIBH respectively; p<0.01).
In stage I, AAA had similar effect on GTV as in stage III. However, differences between the two algorithms were substantial for PTV and more pronounced in DIBH: AAA overestimated all PTV parameters (p<0.01), with largest impact on V45 (up to 41.4% in FB and 66.3% in DIBH), while mean dose and D98 were overestimated by 2.0 Gy and 2.3 Gy in FB and 3.1 Gy and 4.0 Gy in DIBH. These clinically relevant differences may be a combination of small targets and large dose gradients in the SBRT treated volume.
Lung and heart dose parameters decreased in DIBH compared to FB, but were similar for both algorithms and both disease stages (median differences ±0.3% for volumetric parameters and ±0.2 Gy for mean doses). More details on actual dosimetric parameters are presented in the table.